



## 3D-fibroblast tissues constructed by a cell-coat technology enhance tight-junction formation of human colon epithelial cells



Michiya Matsusaki<sup>a</sup>, Daichi Hikimoto<sup>a</sup>, Akihiro Nishiguchi<sup>a</sup>, Koji Kadowaki<sup>a</sup>,  
Kayoko Ohura<sup>b</sup>, Teruko Imai<sup>b</sup>, Mitsuru Akashi<sup>a,\*</sup>

<sup>a</sup> Department of Applied Chemistry, Graduate School of Engineering, Osaka University, 2-1 Yamadaoka, Suita, Osaka, 565-0871, Japan

<sup>b</sup> Department of Pathopharmacology, Graduate School of Pharmaceutical Sciences, Kumamoto University, 5-1 Oe-honmachi, Kumamoto, 862-0973, Japan

### ARTICLE INFO

#### Article history:

Received 16 December 2014

Available online 8 January 2015

#### Keywords:

Caco-2

3D-cell culture

Cell-coat technology

Tight-junction protein

Barrier function

Pharmaceutical application

### ABSTRACT

Caco-2, human colon carcinoma cell line, has been widely used as a model system for intestinal epithelial permeability because Caco-2 cells express tight-junctions, microvilli, and a number of enzymes and transporters characteristic of enterocytes. However, the functional differentiation and polarization of Caco-2 cells to express sufficient tight-junctions (a barrier) usually takes over 21 days in culture. This may be due to the cell culture environment, for example inflammation induced by plastic petri dishes. Three-dimensional (3D) sufficient cell microenvironments similar to *in vivo* natural conditions (proteins and cells), will promote rapid differentiation and higher functional expression of tight junctions.

Herein we report for the first time an enhancement in tight-junction formation by 3D-cultures of Caco-2 cells on monolayered (1L) and eight layered (8L) normal human dermal fibroblasts (NHDF). Trans epithelial electric resistance (TEER) of Caco-2 cells was enhanced in the 3D-cultures, especially 8L-NHDF tissues, depending on culture times and only 10 days was enough to reach the same TEER value of Caco-2 monolayers after a 21 day incubation. Relative mRNA expression of tight-junction proteins of Caco-2 cells on 3D-cultures showed higher values than those in monolayer structures. Transporter gene expression patterns of Caco-2 cells on 3D-constructs were almost the same as those of Caco-2 monolayers, suggesting that there was no effect of 3D-cultures on transporter protein expression. The expression correlation between carboxylesterase 1 and 2 in 3D-cultures represented similar trends with human small intestines. The results of this study clearly represent a valuable application of 3D-Caco-2 tissues for pharmaceutical applications.

© 2015 Elsevier Inc. All rights reserved.

### 1. Introduction

Permeability characteristics of small intestines have been studied widely to characterize the pharmacokinetic properties of drug candidates using human colon carcinoma cell line Caco-2 [1–3]. Caco-2 cells express tight-junctions, microvilli, and a number of enzymes and transporters that are characteristic of enterocytes: peptidases, esterase, P-glycoprotein, uptake transporters for amino acids, bile acids and carboxylic acids [4]. Artursson and co-workers reported a good correlation between oral drug absorption in humans and apparent drug permeability coefficients in Caco-2 cells [5]. Although a relatively long culture period is required for permeability experiments to obtain sufficient barrier

function in Caco-2 cells, until now, the Caco-2 cell monolayer system was the gold standard in pharmaceutical applications. The tight-junction formation (barrier function) of Caco-2 monolayers, which can be detected by trans epithelial electric resistance (TEER) measurements, increase gradually with increasing culture times and reach sufficient barrier function (TEER of over 300  $\Omega \cdot \text{cm}^2$ ) after 21–29 days of incubation [2]. This long-term culture of Caco-2 cells before any experiments is labor intensive and time consuming, which limits versatility and thus limits applicability to pharmaceutical applications [6]. If culture times of Caco-2 cells were shorter, then drug permeability assays using Caco-2 cells would be more widespread.

The necessity of long culture times of Caco-2 cells required to obtain enough barrier functions may be due to traditional cultures on “artificial” plastic substrates. We reported high expressions of heat shock protein 70 (Hsp70) and an inflammatory cytokine 6 (IL-6) from monolayers of human umbilical vein endothelial cells

\* Corresponding author. Fax: +81 6 6879 7359.

E-mail address: [akashi@chem.eng.osaka-u.ac.jp](mailto:akashi@chem.eng.osaka-u.ac.jp) (M. Akashi).

(HUVEC) on tissue culture polystyrene dishes [7]. Hsp70 families are expressed in response to different types of cellular stress, such as elevated heat, mechanical trauma, chemical reagents, and heavy metals [8]. Thus, when cells suffer physical and physicochemical stress from the environment, the production of Hsp70 increases to serve as molecular chaperones in protein folding and transport [9]. IL-6 plays an essential role in intercellular communication, and especially in the inflammatory response [10]. Increase of IL-6 production clearly indicates an inflammatory response in cultured cells on plastic dishes, similar to other reports which represent an induction of inflammation on plastic dishes during the cell culture process [11].

A significant difference between *in vitro* 2D-cultures and *in vivo* tissues or organs is the existence of components surrounding cells, such as extracellular matrices (ECM). In the body, nearly all tissue cells reside in the fibrous nano-meshwork of the ECM, which is typically composed of fibronectin (FN) and collagen, and provides complex biochemical and physical signals [12,13]. Furthermore, *in vivo* tissues or organs are three-dimensional (3D) structures. The 3D-microenvironments consisting of the surrounding ECM and neighboring cells and the signaling of cytokines and growth factors play a significant role in the maturation of cells. Accordingly, 3D-structures of Caco-2 cells consisting of ECM and cells are expected to enhance tight-junction formation (barrier function) during short culture periods.

We developed a simple and unique bottoms-up approach, “a hierarchical cell manipulation technique”, which employs nanometer-sized LbL films consisting of FN and gelatin (G) as a nano-ECM to fabricate 3D-tissue constructs [14–20]. The FN-G nanofilms were prepared directly on cell surfaces, and we discovered that at least 6 nm thick FN-G films acted as a stable adhesive surface for adhesion of the second cell layer. Various 3D-layered constructs consisting of single or multiple types of cells were successfully fabricated such as blood vessel wall structures [19,20]. Recently, we also developed a rapid bottoms-up approach “a cell accumulation technique” by employing a single cell coating using FN-G nanofilms, because the fabrication of two layers (2L) per day is difficult with the technique described above due to the time required for stable cell adhesion [21]. The rapid approach could be used to easily create 3D-tissues over 100  $\mu\text{m}$  thickness after only one day of incubation. Moreover, fully and homogeneously vascularized tissues of 1 cm width and 100  $\mu\text{m}$  height were obtained by a sandwich culture of endothelial cells for one or two days of incubation [21–25]. Notably, we found higher cellular activities and lower inflammatory responses induced from 3D-structures consisting of HUVEC and fibroblast layers as compared to those of monolayer structures [25]. These results motivated us to fabricate 3D-Caco-2 tissue constructs in order to enhance tight-junction formation of Caco-2 cells during short culture periods.

In this study, 3D-multilayered structures consisting of normal human dermal fibroblast (NHDF) and HUVEC were constructed by a cell accumulation technique and their tight-junction formation was evaluated via TEER measurements and messenger RNA (mRNA) expression in relation to the layer number of underlying NHDFs.

## 2. Materials and methods

### 2.1. Materials

Fibronectin (FN) from bovine plasma ( $M_w$   $4.6 \times 10^5$ ) was purchased from Sigma-Aldrich (MO, USA). Gelatin (G) ( $M_w$   $1.0 \times 10^5$ ), tris(hydroxymethyl)aminomethane hydrochloride (Tris-HCl), 10% formalin solution, L-Glutamine, and Dulbecco's modified Eagle's medium (DMEM) were purchased from Wako Pure Chemical Industries (Osaka, Japan). ZO-1 mouse monoclonal antibody, Triton X,

Goat anti-mouse Alexa Fluor 546-conjugated IgG, 4', 6-diamidino-2-phenylindole dihydrochloride (DAPI), fetal bovine serum (FBS), and MEM Non-Essential Amino Acid (NEAA) were purchased from Life Technologies (CA, USA). The 12 well and 24 well cell culture inserts with 0.4  $\mu\text{m}$  pore size were purchased from BD bioscience (NJ, USA) and Corning Inc. (MA, USA). Normal human dermal fibroblast (NHDF) was purchased from Lonza (NJ, USA). Caco-2 was kindly donated by Prof. Imai from Kumamoto University. All of the chemicals were used without further purification.

### 2.2. Construction of Caco-2 3D-tissues

The NHDFs after trypsinization were suspended in 0.04 mg/ml of FN and G/Tris-HCl solution (50 mM, pH = 7.4), and alternately incubated for 1 min using a MicrotubeRotator (MTR-103, AS ONE, Japan) with a washing step. The centrifugation was performed at  $200 \times g$  for 1 min at each step. After 9 steps of coating, about 10 nm of the FN-G nanofilms were coated onto single cell surfaces. The cells were suspended in 1 ml and 0.3 ml of DMEM with 10% FBS, and were seeded onto 12 well and 24 well trans-well inserts with a semipermeable membrane, and 1.5 ml and 1 ml of media was added into the microplates. After 1 h of incubation, another 1 ml of media was added to connect the inner and outside media of the inserts when 24 well inserts were used. The cells were then incubated in 5%  $\text{CO}_2$  at 37 °C. After 1 day, NHDF tissues from a monolayer to 8 layers thickness were constructed. A  $1 \times 10^5$  cells/layer aliquot was used for the 24 well inserts, and  $2.5 \times 10^5$  cells/layer for the 12 well inserts. In the same manner,  $2.5 \times 10^5$  Caco-2 cells were coated with FN-G nanofilms, and were seeded onto each NHDF tissue. The Caco-2 cells adhered within 1 day to form a monolayer Caco-2-3D-NHDF tissues. The medium was changed every other day.

### 2.3. TEER profiles of Caco-2 3D-tissues

TEER of Caco-2 monolayer and 3D-tissues were measured using MILICELL electrical resistance system-2 (Millipore Corp., Bedford, MA). Resistances of blank membrane were subtracted from those of membranes with cells before final resistances were (in  $\Omega \text{ cm}^2$ ) calculated.

### 2.4. RNA isolation and reverse transcription-PCR (RT-PCR)

Total RNA was isolated from cell monolayers using RNAiso reagents (Takara Bio Inc., Shiga, Japan) according to the manufacturer's specifications. First-strand cDNA was synthesized using Oligo(dT) with ReverTra Ace (Toyobo Co., Ltd., Osaka, Japan). The Real-time quantitative PCR reaction was performed in Bio-Rad iCycler iQ real-time PCR detection system (Bio-Rad Laboratories, Inc., Hercules, CA, USA) using SYBR Premix Ex Taq II (Takara Bio Inc.) and primers reported previously [26–28]. Thermal cycling conditions were 95 °C for 1 min, followed by 40 cycles of 95 °C for 10 s, 60 °C for 45 s. Reactions were carried out in triplicate. Relative mRNA levels were calculated using the  $2^{-\Delta\text{Ct}}$  method.

### 2.5. Statistical analysis

Statistical analysis was performed using the unpaired two-tailed Student's *t*-test. All data are represented as means  $\pm$  SD. \*,  $P < 0.05$ ; \*\*,  $P < 0.01$ . N.S. means no significant difference.

### 3. Results and discussion

#### 3.1. Construction of 3D-Caco-2 tissues

Caco-2 monolayer, monolayered (1L) Caco-2-1L NHDFs (1L-1L), and 1L Caco-2-eight-layered (8L) NHDFs (1L-8L) were constructed in cell culture inserts and then expressed tight-junction protein ZO-1 was immunologically labeled for observation via confocal laser scanning microscopy (CLSM) (Fig. 1). Homogenous flat fluorescent expression was observed in Caco-2 monolayers, whereas fluorescent expression of 1L-1L and 1L-8L structures were not flat, probably due to surface roughness. Although surfaces of cell culture inserts are smooth, 1L or 8L-NHDFs surfaces are not smooth because of sloping cell surfaces. Actually when the focal plane of CLSM was changed in the Z direction, ZO-1 expression was observed clearly throughout the area. This trend was remarkable in 1L-8L structures. Schematic illustrations of all samples are described in Fig. 1. 3D-reconstructed CLSM images of 1L-8L constructs indicated roughness in top surfaces as shown in the Supplementary Information (Supplementary Fig. S1).

#### 3.2. TEER profiles of 3D-Caco-2 tissues

In order to optimize the cell number of Caco-2 for tight-junction expression, the seeding cell number was changed from  $0.625 \times 10^5$ ,  $1.25 \times 10^5$  cells in 12-well cell culture inserts (cell densities are  $0.56$ ,  $1.1$ , and  $2.2 \times 10^5$  cells/cm<sup>2</sup>) because cell densities of  $2.0$ – $2.5 \times 10^5$  cells/cm<sup>2</sup> have been widely used for permeability assays [2]. TEER profiles of the highest cell densities dramatically increased to the maximum value  $550 \Omega \text{ cm}^2$  at day 7, suddenly decreased to  $200 \Omega \text{ cm}^2$  until day 19, and then gradually increased to  $300 \Omega \text{ cm}^2$  until day 35 (Fig. 2a). The strange increase of the highest cell density at an early period might be due to the temporal formation of cell aggregation, and subsequent detachment of the cell aggregation would induce drastic decrements in the TEER value until day 19. After the detachment, the TEER value gradually increased with accompanying growth of the remaining Caco-2 cells until confluence was achieved. On the other hand,  $0.625$  and  $1.25 \times 10^5$  seeding cell numbers showed almost the same profile, gradually increased and reached a maximum value  $350 \Omega \text{ cm}^2$  at

day 25 and then maintained the max value until day 35. It was the same profile as the previously reported TEER profile [26–28], and thus  $0.625 \times 10^5$  cell number ( $0.56 \times 10^5$  cells/cm<sup>2</sup>) was used for further experiments of Caco-2 monolayers.

Interestingly, TEER profiles of 1L-8L revealed a continuous increase with increasing culture times and reached  $350 \Omega \text{ cm}^2$  at day 10, whereas Caco-2 monolayers need 25 day of incubation to reach the highest  $350 \Omega \text{ cm}^2$  value (Fig. 2B). Furthermore, the TEER value of 1L-8L continuously increased after day 10 and was maintained at a high level, approximately  $400$ – $450 \Omega \text{ cm}^2$ , until day 28. The 1L-1L structures also showed higher TEER values than those of Caco-2 monolayer and reached a maximum of  $300 \Omega \text{ cm}^2$  on day 12. Since NHDF layers did not show any TEER values, these higher barrier properties were assigned to Caco-2 layers on 3D-NHDF multilayers clearly. Actually, the permeability of lucifer yellow of 3D-constructs was much lower than Caco-2 monolayers and permeability of fluorescent molecules were not observed after 3 days of incubation (Supplementary Information Fig. S2). These data encouraged us to study in detail the mRNA expression of tight-junction proteins during 3D-culture periods.

#### 3.3. mRNA expression of tight-junction proteins in 3D-Caco-2 tissues

The gene expression of four proteins, Occludin, Zonula Occludens (ZO)-1, Tricellulin, and Claudin-4, were selected because they are important proteins for tight-junction formation [29]. Since a  $300 \Omega \text{ cm}^2$  TEER value is a criteria commonly used for permeability assays [26–28], we collected mRNA of all samples on day 12 because the TEER value of 1L-1L samples reached  $300 \Omega \cdot \text{cm}^2$  on day 12. Notably the TEER value at day 12 of 1L-8L structures was  $383 \Omega \cdot \text{cm}^2$ , whereas that of Caco-2 monolayers was almost half the value at  $160 \Omega \cdot \text{cm}^2$ . To evaluate the stability of the barrier function, mRNA was also collected 1 week later (day 19).

Before real-time polymerase chain reaction (PCR) experiments, we expected that gene expressions of 3D-samples, 1L-1L and 1L-8L, would be higher than that of monolayers, due to their higher TEER values. However, actual gene expression patterns were completely opposite, Caco-2 monolayers showed approximately ten-times higher expressions than those of 3D-samples at both dates (Fig.

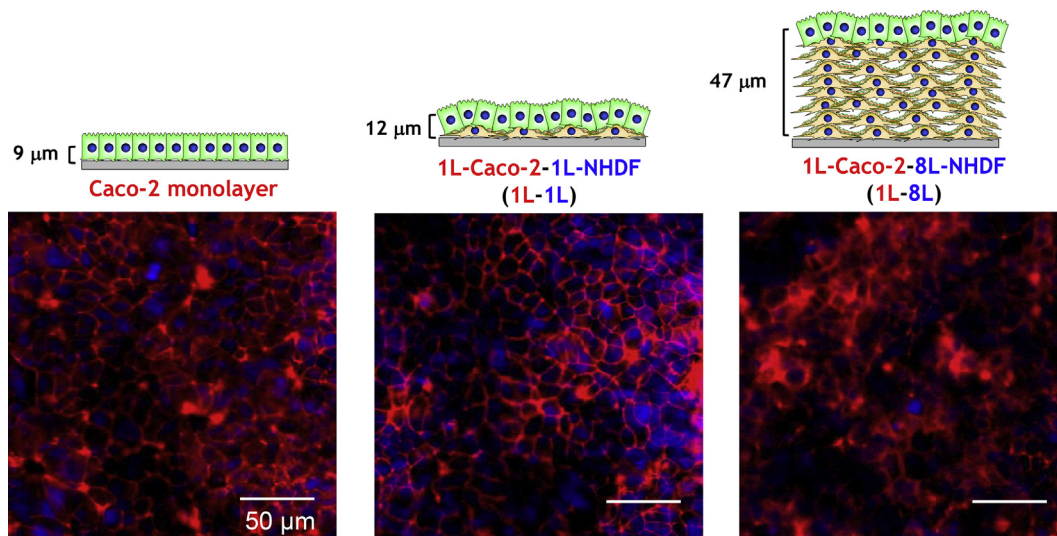


**Fig. 1.** Schematic illustration of Caco-2 monolayers (top left) and 3D-constructs consisting of monolayers (1L) Caco-2 and 1L-normal human dermal fibroblast (NHDF) cells (top center) or 8L-NHDF (top right). Confocal laser scanning microscopy (CLSM) images of samples stained with Alexa546-labeled anti ZO-1 antibodies (red) and DAPI stain (blue) (bottom). Samples were cultured at 37 °C for 12 days in DMEM with 10% FBS. (For interpretation of the references to color in this figure legend, the reader is referred to the web version of this article.)

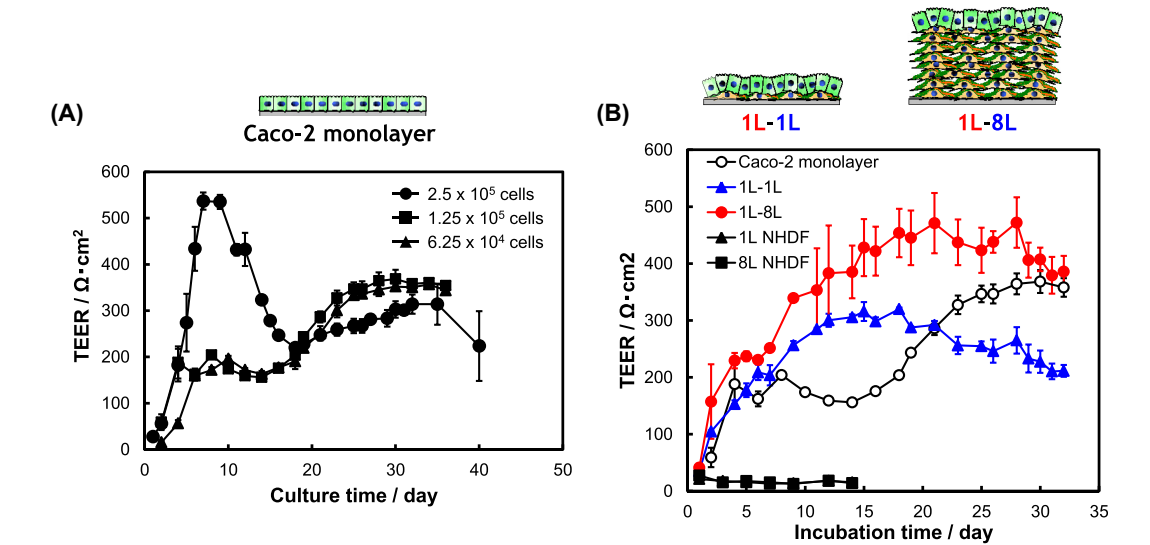


**Fig. 2.** Trans epithelial electric resistance (TEER) profiles of Caco-2 monolayers with different seeding cell numbers (A) and 3D-constructs with 1L-1L and 1L-8L structures (B) for over a month in DMEM with 10% FBS (n = 3). Caco-2 monolayers were prepared at 6.25 × 10<sup>4</sup> cells conditions and 1L and 8L-NHDFs were also used as controls.

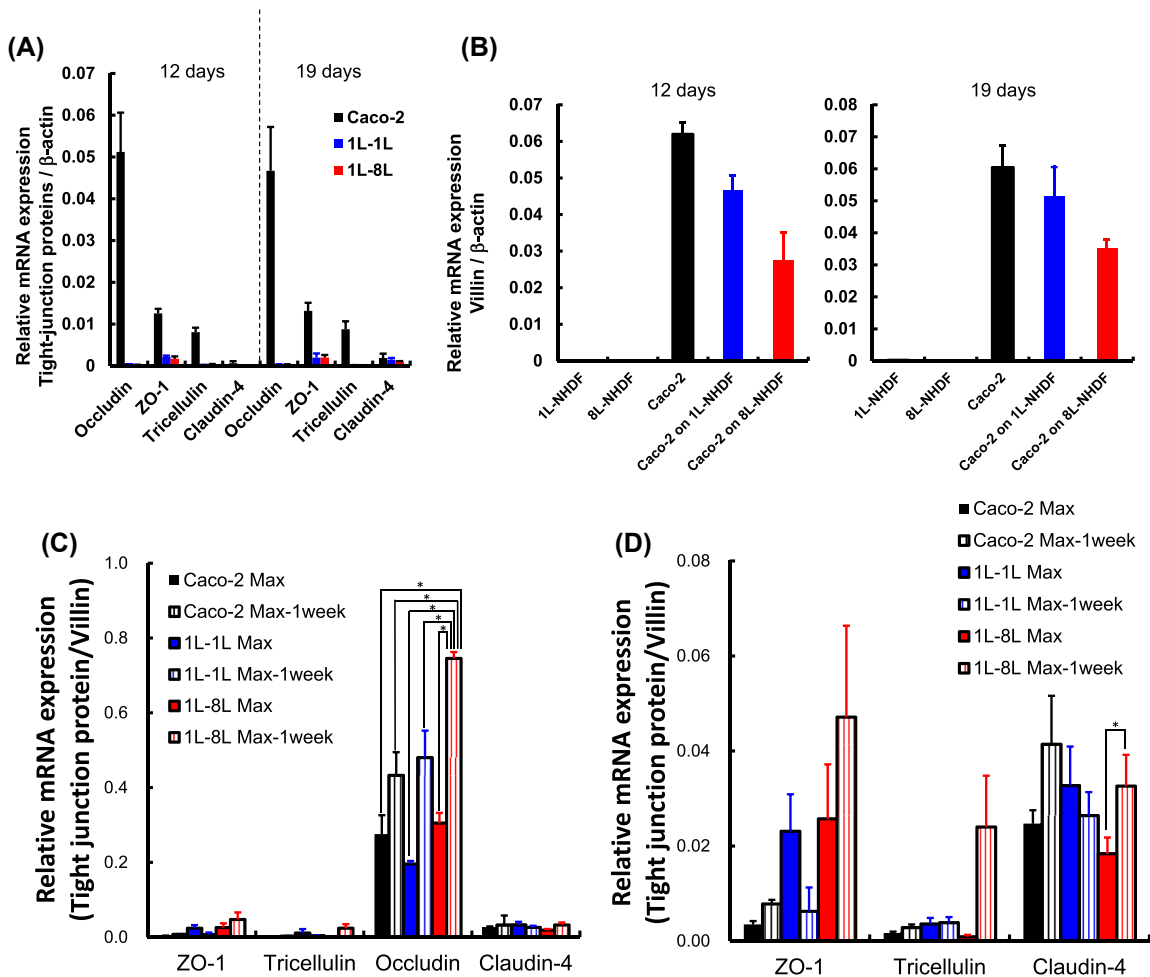


**Fig. 3.** Relative mRNA expression of tight junction proteins of Caco-2 monolayers and 3D-constructs after 12 and 19 days cultures by real-time polymerase chain reactions (PCR) using β-actin as a house keeping gene (n = 3) (A). The relative mRNA expression of villin protein after 12 and 19 days cultures by real-time-PCR using β-actin as a house keeping gene (n = 3) (B). The relative mRNA expression of tight junction proteins of Caco-2 monolayers and 3D-constructs by real-time-PCR using villin as a house keeping gene (n = 3) (C). The relative mRNA expression data except Occludin (D). Sample DNA was collected at the day of the maximum TEER value (Max) and 1 week more (Max-1week). Max and Max-1 week of Caco-2 monolayers were 21 and 28 days and Max and Max-1 week of 3D-constructs are 14 and 21 days, respectively.



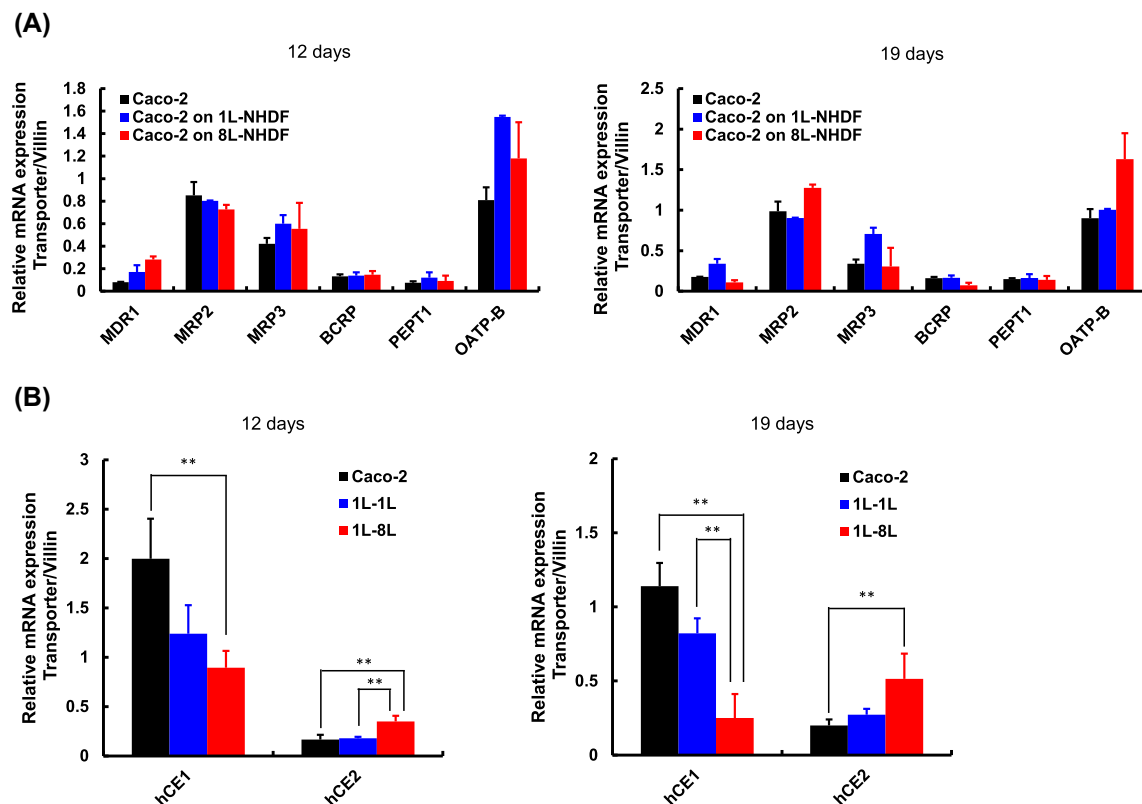
3A). Unexpected results arose from expressed amounts of house-keeping genes. The mRNA expression of  $\beta$ -actin, which is a widely-used house-keeping gene, was used in this study, but this gene was also expressed in NHDF because  $\beta$ -actin, non-muscle cytoskeletal actin, was usually expressed in all adherent cells. Accordingly, gene expression patterns of tight-junction proteins of Caco-2 cells were diluted with a large amount from the  $\beta$ -actin gene in underlying NHDFs cells. In order to resolve this issue, we focused on actin-binding protein, villin, which is specifically expressed in the brush border of the epithelium [30]. If we use villin as a house-keeping gene, gene expression of tight-junction proteins of Caco-2 will be estimated selectively. Fig. 3B indicates the relative mRNA expression of villin of all samples against  $\beta$ -actin. As we expected, 1L- or 8L-NHDF did not express any villin, while Caco-2 monolayers and 3D-structures clearly expressed villin. The gene expression of 3D-structures was slightly lower than in monolayers, but was clearly confirmed. Based on gene expression data, we tried to evaluate tight-junction protein expression against villin.

Fig. 3 shows relative mRNA expression of tight-junction proteins in all samples using villin expression as a house-keeping gene. In this experiment, mRNA was collected on the day of the maximum TEER value (Max) and 1 week later (Max-1week) in order to evaluate the effect of 3D-structures against monolayers on barrier functions of Caco-2. For example, Max and Max-1week of 3D-samples were day 14 (1L-1L: 305  $\Omega$  cm<sup>2</sup> and 1L-8L: 385  $\Omega$  cm<sup>2</sup>) and 21 (1L-1L: 292  $\Omega$  cm<sup>2</sup> and 1L-8L: 471  $\Omega$  cm<sup>2</sup>) and Max and Max-1week of Caco-2 monolayers were day 21 (292  $\Omega$  cm<sup>2</sup>) and 28 (364  $\Omega$  cm<sup>2</sup>), respectively. Gene expressions of Occludin were about ten-times higher than those of other tight-junction proteins (Fig. 3A). The Max values were almost the same level, but Max-1week of 1L-8L revealed a significantly higher value than in the others, probably due to the correlation with the highest TEER value. When

we focused on the other tight-junction proteins, higher gene expression patterns were observed on 1L-1L and 1L-8L structures (Fig. 3B). Notably ZO-1 expressions of 3D-structures were five-to ten-times higher than those of monolayers. The results of these studies suggested that 3D-structures were effective in tight-junction formation of Caco-2, and accelerated the expression of tight-junction proteins by at least 1 week against monolayers.

### 3.4. mRNA expressions of transporter proteins and carboxylesterase of 3D-Caco-2 tissues

Transporters localized in the cytoplasmic membrane are important proteins for moving nutrients, drugs, or toxic substances. Especially, drug efflux transport systems (MDR1, MRP2, MRP3, BCRP, and PEPT1) such as the ATP-dependent efflux transporter (P-glycoprotein) are responsible for moving compounds like neurotransmitters, toxic substances, and antibiotics, out of cells, and this is considered to be a vital part of xenobiotic metabolism [31,32]. Influx transporters (PEPT1 and OATP-B) are not only responsible for bringing in needed nutrients into the cell, but are also necessary for the intracellular movement of medications where they will be brought into contact with enzymes responsible for their metabolism and preparation for elimination or possibly to exert their therapeutic or biologic effect. Thus, we evaluated relative mRNA expressions of transporters of 3D-structures against Caco-2 monolayers (Fig. 4A). All gene expressions of both efflux and influx transporters of 3D-structures at day 12 and 19 are the same level as those of monolayers, suggesting that there are no significant effects of 3D-culture on the expression of transporter proteins. In other words, 3D-constructs with 1L or 8L-NHDFs did not affect the expression of transporter proteins of Caco-2.



**Fig. 4.** The relative mRNA expression of transporter proteins of Caco-2 monolayers and 3D-constructs after 12 and 19 days by realtime-PCR using villin as a house keeping gene ( $n = 3$ ) (A). Relative mRNA expression of carboxylesterase 1 and 2 (hCE1 and hCE2) of Caco-2 monolayers and 3D-constructs after 12 and 19 days by realtime-PCR using villin as a house keeping gene ( $n = 3$ ) (B).

Finally, we evaluated mRNA expression of human carboxylesterase 1 (hCE1) and 2 (hCE2) which are serine esterases involved in both drug metabolism and activation [33]. hCE1 mainly hydrolyzes a substrate with a small alcohol group and large acyl group, but its wide active pocket sometimes allows it to act on structurally distinct compounds of either large or small alcohol moieties. In contrast, hCE2 recognizes a substrate with a large alcohol group and a small acyl group, and its substrate specificity may be restricted by a capability of acyl-hCE2 conjugate formation due to the presence of conformational interference in the active pocket. Regarding drug absorption, the expression pattern of hCE1 and hCE2 in Caco-2 monolayers (higher expression of hCE1 and lower expression of hCE2) is completely different from that in the human small intestine (lower expression of hCE1 and higher expression of hCE2) [33,34]. Therefore, the prediction of human intestinal absorption using Caco-2 monolayer should be careful in the case of ester and amide-containing drugs or prodrugs. Accordingly, if 3D-structures of Caco-2 can change the expression correlation between hCE1 and hCE2 same as that in the human small intestine, it will open new windows in the Caco-2 application for the prediction of drug absorption.

Relative mRNA expression of hCE1 of Caco-2 monolayer at day 12 and 19 was ten-times higher than that of hCE2, and these phenomena tended to corroborate the report of Sun and co-workers (Fig. 4B) [34]. Interestingly, the expression of hCE1 decreased with increasing the layer number of NHDFs and hCE1 expression of 1L–8L at day 19 was approximately five-times lower than that of Caco-2 monolayers. In contrast, hCE2 expressions in 3D-structures were slightly higher than in Caco-2 monolayers and the expression of 1L–8L at day 19 was approximately 2.5-times higher than that of the monolayer. These results clearly suggest that 3D-construction using Caco-2 and NHDFs has a significant potential to improve Caco-2 properties to analogous properties of the human small intestine.

In conclusion, we report for the first time the fabrication of 3D-tissue constructs consisting of Caco-2 and multilayered NHDFs. 3D-structures enhanced barrier functions corresponding to the expression of tight-junction proteins, and accelerated expression of tight-junction proteins at least 1 week against monolayers. 3D-constructs with 1L or 8L-NHDFs did not affect the expression of transporter proteins of Caco-2, and efflux and influx transporters expressed at the same level as those of Caco-2 monolayers. Notably, the expression correlation of hCE1 and hCE2 in 3D-structures was almost the same as in the human small intestine, suggesting a significant potential to improve hCE expression properties of Caco-2 cells against monolayer cultures. This study reveals a valuable novel application of 3D-Caco-2 tissues for pharmaceutical applications.

## Conflict of interest

There is no conflict of interest.

## Acknowledgments

This work was mainly supported by the Funding Program for Next Generation World-Leading Researchers (NEXT Program: LR026) and partially by a Grant-in-Aid for Scientific Research (S) (A232250040) from the Japan Society for the Promotion of Science (JSPS) and by the SENTAN-JST program (13A1204).

## Appendix A. Supplementary data

Supplementary data related to this article can be found at <http://dx.doi.org/10.1016/j.bbrc.2014.12.118>.

## References

- [1] I.J. Hidalgo, T.J. Raub, R.T. Borchardt, Characterization of the human colon carcinoma cell line (Caco-2) as a model system for intestinal epithelial permeability, *Gastroenterology* 96 (1989) 738–749.
- [2] I. Hubatsch, E.G.E. Ragnarsson, P. Artursson, Determination of drug permeability and prediction of drug absorption in Caco-2 monolayers, *Nat. Prot.* 2 (2007) 2111–2119.
- [3] J.M. Gamboa, K.W. Leong, In vitro and in vivo models for the study of oral delivery of nanoparticles, *Adv. Drug. Deliv. Rev.* 65 (2013) 800–810.
- [4] M. Pinto, et al., Enterocyte-like differentiation and polarization of the human colon carcinoma cell line Caco-2 in culture, *Biol. Cell.* 47 (1983) 323–330.
- [5] P. Artursson, J. Karlsson, Correlation between oral drug absorption in humans and apparent drug permeability coefficients in human intestinal epithelial (Caco-2) cells, *Biochem. Biophys. Res. Commun.* 175 (1991) 880–885.
- [6] Y. Cai, C. Xu, P. Chen, et al., Development, validation, and application of a novel 7-day Caco-2 cell culture system, *J. Pharm. Tox. Methods* 70 (2014) 175–181.
- [7] K. Kadowaki, M. Matsusaki, M. Akashi, Three-dimensional constructs induce high cellular activity: structural stability and the specific production of proteins and cytokines, *Biochem. Biophys. Res. Commun.* 402 (2010) 153–157.
- [8] M. Ashburner, J.J. Bonner, The induction of gene activity in drosophila by heat shock, *Cell* 17 (1979) 241–254.
- [9] J.G. Kiang, G.C. Tsokos, Heat shock protein 70 kDa: molecular biology, biochemistry, and physiology, *Pharmacol. Ther.* 80 (1998) 183–201.
- [10] S.J. Van, Interleukin-6: an overview, *Annu. Rev. Immunol.* 8 (1990) 253–278.
- [11] S. Sawada, S. Sakaki, Y. Iwasaki, et al., Suppression of the inflammatory response from adherent cells on phospholipid polymers, *J. Biomed. Mater. Res.* 64A (2003) 411–416.
- [12] N.J. Boudreau, P.L. Jones, Extracellular matrix and integrin signalling: the shape of things to come, *Biochem. J.* 339 (1999) 481–488.
- [13] R.O. Hynes, Fibronectins, Springer-Verlag Inc, New York, 1990.
- [14] M. Matsusaki, K. Kadowaki, Y. Nakahara, et al., Fabrication of cellular multi-layers with nanometer-sized extracellular matrix films, *Angew. Chem. Int.* 46 (2007) 4689–4692.
- [15] M. Matsusaki, H. Ajiro, T. Kida, et al., Layer-by-layer assembly through weak interactions and their biomedical applications, *Adv. Mater.* 24 (2012) 454–474.
- [16] M. Matsusaki, S. Amemori, K. Kadowaki, et al., Quantitative 3D analysis of nitric oxide diffusion in a 3D artery model using sensor particles, *Angew. Chem. Int.* 50 (2011) 7557–7561.
- [17] H. Hosoya, K. Kadowaki, M. Matsusaki, et al., Engineering fibrotic tissue in pancreatic cancer: a novel three-dimensional model to investigate nanoparticle delivery, *Biochem. Biophys. Res. Commun.* 419 (2012) 32–37.
- [18] P. Chetprayoon, K. Kadowaki, M. Matsusaki, et al., Survival and structural evaluations of three-dimensional tissues fabricated by the hierarchical cell manipulation technique, *Acta Biomater.* 9 (2012) 4698–4706.
- [19] M. Matsusaki, K. Kadowaki, E. Adachi, et al., Morphological and histological evaluations of 3D-layered blood vessel constructs prepared by hierarchical cell manipulation, *J. Biomater. Sci. Polym.* 23 (2012) 63–79.
- [20] R. Ishiwata, U. Yokoyama, M. Matsusaki, et al., Three-dimensional multilayers of smooth muscle cells as a new experimental model for vascular elastic fiber formation studies, *Atherosclerosis* 233 (2014) 590–600.
- [21] A. Nishiguchi, H. Yoshida, M. Matsusaki, et al., Rapid construction of three-dimensional multilayered tissues with endothelial tube networks by the cell-accumulation technique, *Adv. Mater.* 23 (2011) 3506–3510.
- [22] M. Matsusaki, Development of three-dimensional tissue models based on hierarchical cell manipulation using nanofilms, *Bull. Chem. Soc. Jpn.* 85 (2012) 401–414.
- [23] A. Nishiguchi, M. Matsusaki, Y. Asano, et al., Effects of angiogenic factors and 3D-microenvironments on vascularization within sandwich culture, *Bio-materials* 35 (2014) 4739–4748.
- [24] Y. Asano, A. Nishiguchi, D. Okano, et al., Ultrastructure of blood and lymphatic vascular networks in three-dimensional cultured tissues fabricated by ECM nanofilm-based cell accumulation technique, *Microscopy* 63 (2014) 219–226.
- [25] M. Matsusaki, C.P. Case, M. Akashi, Three-dimensional cell culture technique and pathophysiology, *Adv. Drug Deliv. Rev.* 74 (2014) 95–103.
- [26] N. Wang, Y. Wang, P. Li, et al., The bioavailability of hepatoprotective flavonoids in hypericum japonicum extract, *J. Bioanal. Biomed.* 1 (2009) 33–38.
- [27] P. Artursson, Epithelial transport of drugs in cell culture. I: a model for studying the passive diffusion of drugs over intestinal absorptive (Caco-2) cells, *J. Pharm. Sci.* 79 (1990) 476–482.
- [28] F. Leonard, E.M. Collnot, C.M. Lehr, A three-dimensional coculture of enterocytes, monocytes and dendritic cells to model inflamed intestinal mucosa in vitro, *Mol. Pharm.* 7 (2010) 2103–2119.
- [29] S. Tsukita, M. Furuse, Claudin-based barrier in simple and stratified cellular sheets, *Curr. Opin. Cell. Biol.* 14 (2002) 531–536.
- [30] A. Bretscher, K. Weber, Villin: the major microfilament-associated protein of the intestinal microvillus, *Proc. Natl. Acad. Sci. U. S. A.* 76 (1979) 2321–2325.
- [31] R.B. Kim, Transporters and xenobiotic disposition, *Toxicology* 181 (2002) 291–297.

- [32] M.J. Dresser, M. Kaushal, K. Leabman, et al., Transporters involved in the elimination of drugs in the kidney: organic anion transporters and organic cation transporters, *J. Pharm. Sci.* 90 (2001) 397–421.
- [33] T. Imai, Human carboxylesterase isozymes: catalytic properties and rational drug design, *Drug Metab. Pharmacokinet.* 21 (2006) 173–185.
- [34] D. Sun, H. Lennernas, L.S. Welage, et al., Comparison of human duodenum and Caco-2 gene expression profiles for 12,000 gene sequences tags and correlation with permeability of 26 drugs, *Pharm. Res.* 19 (2002) 1400–1416.